Desalination and Water Treatment
www.deswater.com

doi: 10.5004/dwt.2021.27619

234 (2021) 245–254
September

Adsorptive removal of methyl orange from wastewaters by the commercial anion exchange membrane EPTAC

Muhammad Imran Khan[a,*], Abdallah Shanableh[a], Nida Nasir[a], Shabnam Shahida[b]

[a]*Research Institute of Sciences and Engineering, University of Sharjah, Sharjah 27272, United Arab Emirates, emails: raoimranishaq@gmail.com/mimran@sharjah.ac.ae (M. Imran Khan), shanableh@sharjah.ac.ae (A. Shanableh), nnasir@sharjah.ac.ae (N. Nasir)*

[b]*Department of Chemistry, University of Poonch, Rawalakot 12350, Azad Kashmir, Pakistan, email: shabnamshahida@upr.edu.pk*

Received 4 April 2021; Accepted 15 July 2021

ABSTRACT

In this manuscript, we have utilized the commercially available anion exchange membrane EPTAC for the adsorptive removal of methyl orange (MO) dye from wastewater via batch mode at room temperature. The percentage removal of MO was increased from 26.10% to 98.70% with the contact time, and from 48.04% to 98.70% with the amount of adsorbent (membrane dosage). On the other hand, the percentage removal of MO was decreased with an initial concentration of dye aqueous solution, temperature and ionic strength. Adsorption kinetics evaluation showed that experimental data for adsorption of MO onto the commercial anion exchange membrane EPTAC fitted-well to pseudo-second-order model because the value of correlation coefficient (R^2) was very close to unit ($R^2 > 0.995$). Several nonlinear isotherms containing two parameters and three parameters isotherms were applied on experimental data of MO adsorption onto the commercial anion exchange membrane EPTAC. Results demonstrated that adsorption MO onto the commercial anion exchange membrane EPTAC fitted well to nonlinear Freundlich isotherm with the lower value of chi-square ($\chi^2 = 2.22 \times 10^{-9}$) Moreover, adsorption thermodynamics of MO adsorption onto the commercial anion exchange membrane EPTAC was also evaluated in detail. The negative value of enthalpy of the system ($\Delta H° = -68.93$ kJ/mol) showed that adsorption of MO onto the commercial anion exchange membrane EPTAC was an exothermic process.

Keywords: Anion exchange membrane EPTAC; Exothermic process; Pseudo-second-order model; Methyl orange; Nonlinear isotherms

1. Introduction

Different synthetic dyes employed in several industries namely textile, leather, paint, and so forth produce the highly visible wastewater effluents [1,2]. Some of them are dangerous and cause a serious threat to the environment. The discharge of dyes into canals, rivers, etc. even in a minor quantity can affect aquatic life. Azo dyes are most largely employed for natural and synthetic fiber dyeing and printing and also in paints, plastics, rubber, and so on. Under special conditions, they can decompose to produce about 20 types of carcinogenic aromatic amines and change human DNA structure to result in induced lesions and cancer [3]. Wastewaters with azo dyes are extensively discharged, and azo dyes are normally present in high concentration and varied compositions. Some recent research takes sulfonated azo-dye methyl orange (MO) as a model dye which is the most commonly employed substance as an acid–base indicator [4–7]. The study of the removal of MO from aqueous solution may be beneficial for more research and practical uses in azo-dye wastewater treatment.

To date, a lot of methods such as electro-oxidation, advanced oxidation processes, coagulation and flocculation,

---

* Corresponding author.

adsorption, biological degradation and membranes processes have been employed for decoloration and degradation of dyestuff from wastewater. Adsorption is the most useful method for color removal due to its simplicity, high efficiency, and ease of operation as well as the availability of a wide range of adsorbents.

Many kinds of materials were therefore investigated as the possible alternatives [8], such as the use of natural materials (kaolinite [9,10], wood [11]), rice husk [12–14], plant leaves [15–18] and agriculture/industrial solid wastes (coconut husk [19,20] maize cob [21] Fe(III)/Cr(III) hydroxides [22]) as easily available, cost-effective, ion exchange membranes (IEMs) [23], and eco-friendly adsorbents. Their price and efficiency vary from one adsorbent to other.

Previously, we have studied the adsorptive removal of congo red from wastewaters by using powder of different plant leaves such as Bougainvillea glabra [15], Morus alba [18], Citrus sinensis [17], and Syzygium cumini [16], as bioadsorbents. Adsorption of different metal ions including lanthanum [14], cerium [12], nickel [13], cobalt [24], copper [25] was investigated by using rise husk as bioadsorbent. Moreover, the adsorption of anionic dyes onto ion-exchange membranes (IEMs) (especially anion exchange membranes) was also evaluated [26,27]. To extend our work, we used the commercial anion exchange membrane EPTAC as an outstanding adsorbent for the removal of MO from wastewaters. To the best of my knowledge, adsorption of MO onto the commercial anion exchange membrane EPTAC was not explored yet.

In this manuscript, adsorption of MO from wastewaters onto the commercial anion exchange membrane EPTAC was carried out at room temperature. The effect of operating parameters on the percentage removal of MO was also investigated. Adsorption kinetics for adsorption of MO onto the commercial anion exchange membrane EPTAC was explored by using several kinetic models such as pseudo-first-order model, pseudo-second-order model, Elovich model, liquid film diffusion model, modified Freundlich equation and Bangham equation. An adsorption isotherms study for adsorption of MO was carried out by employing the nonlinear method. Moreover, adsorption thermodynamics was also investigated for adsorption of MO onto the commercial anion exchange membrane EPTAC.

2. Experimental

2.1. Adsorbent

The commercial anion exchange membrane EPTAC was kindly provided by ChemJoy Membrane Co., Ltd., Hefei, Anhui, P.R. China. Its ion exchange capacity and water uptakes are 0.42 mmol/g and 164.31% respectively.

2.2. Adsorbate

Methyl orange (MO) dye was supplied by Fluka Chemicals (United States of America). It was employed as adsorbate in this research. Sodium chloride (NaCl) was received from Sinopharm Chemical Reagent Co. Ltd., Shanghai, P.R. China. All the chemicals were used as received. Distilled water was used throughout the work. The chemical structure of MO is depicted in Fig. 1.

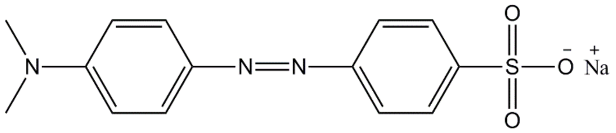

Fig. 1. Chemical structure of methyl orange (MO) dye.

2.3. Batch adsorption test

Herein, batch adsorption of MO from wastewater onto the commercial anion exchange membrane EPTAC was carried out as described [26–31]. Initially, the solution of MO was prepared by dissolving a measured amount of MO into deionized water at ambient temperature. The optimized contact time was determined by shaking the measured amount of EPTAC (0.1) into 40 mL of MO solution with an initial concentration of 50 mg/L at room temperature with different time intervals such as 30, 60, 90, 180, 240, 360, 600, 900 and 1,440 min. To determine the optimized amount of the commercial anion exchange membrane EPTAC (dosage), the different amounts of the EPTAC such as 0.02. 0.04, 0.06, 0.08 and 0.10 g were shaken into 40 mL of MO solution with an initial concentration of 50 mg/L for 1,440 min at room temperature. Adsorption isotherm study was carried out by shaking the EPTAC (0.10 g) for 1,440 min at ambient temperature into 40 mL MO solution with an initial concentration of 100, 200, 300, 400, and 500 mg/L. The influence of ionic strength on adsorption of MO onto the commercial anion exchange membrane EPTAC was investigated by using different concentrations of NaCl such as 0.2, 0.5, 0.8, 1.0, and 1.5 M with shaking speed of 120 rmp, contact time of 1,440 min and membrane dosage of 0.10 g. To study adsorption thermodynamics, 40 mL MO solution with an initial concentration of 50 mg/L was employed and the membrane was shaken at 293, 313, 313 and 323 K for 1,440 min with a constant membrane dosage of 0.10 g and stirred at speed of 120 rmp. The UV-Vis spectrophotometer (UV-2550, Shimadzu, Kyoto, Japan) was used to determine the concentration of MO by determining the absorbance of the supernatant at the wavelength (λ_{max} = 464 nm for MO). The concentration of MO was determined from the calibration curve. The MO adsorbed onto the commercial anion exchange membrane EPTAC at time *t*, was calculated by using Eq. (1).

$$q_t = \frac{C_o - C_t}{W} \times V \tag{1}$$

where C_o and C_t represent the concentration of MO at the initial state and at time *t* respectively. Similarly, *V* and *W* are the volumes of MO aqueous solution and weight of membrane respectively.

2.4. Adsorption kinetics

Adsorption kinetics for MO adsorption onto the anion exchange membrane EPTAC was studied in detail by employing several kinetic models including pseudo-first-order model, pseudo-second-order model, Elovich model, liquid film diffusion model, modified Freundlich equation and Bangham equation. Their detail is given below:

2.4.1. Pseudo-first-order model

The Lagergren pseudo-first-order rate in linear form is represented as [12,16,17]:

$$\log\left(q_e - q_t\right) = \log q_e - \frac{K_1 t}{2.303} \tag{2}$$

where k_1 (min^{-1}), q_e and q_t are rates constant of pseudo-first-order model, the concentration of MO adsorbed at equilibrium and time t respectively.

2.4.2. Pseudo-second-order model

The pseudo-second-order kinetic model in linearized form is represented as [18,28,32]:

$$\frac{t}{q_t} = \frac{1}{k_2 q_e^2} + \frac{t}{q_e} \tag{3}$$

where k_2 (g/mg min) is the rate constant of the pseudo-second-order model.

2.4.3. Elovich model

The Elovich model is expressed as [33,34]:

$$q_t = \frac{1}{\beta}\ln\left(\alpha\beta\right) + \frac{1}{\beta}\ln t \tag{4}$$

where α (mg/g min) and β (g/mg) are constant. The parameter α is the initial adsorption rate and β is the extent of surface coverage and activation energy for chemisorption.

2.4.4. Liquid film diffusion model

It is expressed as:

$$\ln\left(1 - F\right) = -K_{\text{fd}} t \tag{5}$$

where K_{fd} is liquid film diffusion rate constant, and $F = q_t/q_e$.

2.4.5. Modified Freundlich equation

It was originally developed by Kuo and Lotse [26,30]

$$q_t = kC_o t^{1/m} \tag{6}$$

where k, C_o, t and m are adsorption rate constant (L/g min), initial concentration (mg/L), contact time (min) and the Kuo–Lotse constant respectively. Its linear form is shown as:

$$\ln q_t = \ln\left(kC_o\right) + \frac{1}{m}\ln t \tag{7}$$

2.4.6. Bangham equation

Bangham equation is shown as [26,30]:

$$\log\log\left(\frac{C_o}{C_o - q_t m}\right) = \log\left(\frac{k_o m}{2.303V}\right) + \alpha \log t \tag{8}$$

where m is the weight of the anion exchange membrane utilized (g/L), V is the volume of dye solution (mL), α (<1) and k_o (mL/(g/L)) are constants.

2.5. Adsorption isotherms

Experimental data for adsorption of MO onto the commercial anion exchange membrane EPTAC was subjected to various nonlinear isotherms such as two-parameter isotherms (Langmuir, Freundlich, Temkin, Dubinin–Radushkevich (D–R)) and three-parameter isotherms (Hill, Redlich–Peterson and Sips). The details are given as follows:

2.5.1. Two-parameters adsorption isotherms

Herein, Langmuir, Freundlich, Dubinin–Radushkevich (D–R) and Temkin isotherms were employed to evaluate adsorption of MO onto the commercial anion exchange membrane EPTAC.

Nonlinear Langmuir isotherm model is expressed as [26]:

$$q_e = \frac{Q_m k_L C_e}{1 + k_L C_e} \tag{9}$$

where k_L is Langmuir constant (L/mol) and Q_m is Langmuir monolayer adsorption capacity (mol/g).

Nonlinear Freundlich isotherm model is expressed as [26]:

$$q_e = K_f C_e^{1/n} \tag{10}$$

where C_e is the supernatant concentration at equilibrium state of the system (mol/L), and q_e is the amount of dye adsorbed at equilibrium state of the system (mol/g), K_f and n are Freundlich parameters.

D–R model was utilized to distinguish between physical and chemical adsorption processes [26,35]. It is given by the below equation:

$$q_e = C_m \exp\left(-\beta\varepsilon^2\right) \tag{11}$$

ε is the Polanyi potential that is given as:

$$\in = RT\ln\left(1 + \frac{1}{C_e}\right) \tag{12}$$

where R is the universal gas constant (kJ/mol) and T is the absolute temperature (K). β is related to the mean adsorption energy by the below relationship.

$$E = \frac{1}{\sqrt{2\beta}} \tag{13}$$

Temkin isotherm is expressed as [26]:

$$q_e = \frac{RT}{b_T}\ln\left(a_T C_e\right) \tag{14}$$

where b_T is related to the heat of adsorption and a_T is the equilibrium binding constant coinciding with the maximum binding energy.

2.5.2. Three-parameters adsorption isotherms

Experimental data for the adsorption of MO onto the EPTAC was also subjected to three-parameter isotherm models including, Hill, Redlich–Peterson and Sips which denote adsorption capacity as a characteristic function of equilibrium concentration and are empirical in nature [26].

The nonlinear Hill adsorption isotherm is given as:

$$q_e = \frac{q_H C_e^{n_H}}{k_H + C_e^{n_H}} \tag{15}$$

Redlich–Peterson isotherm contains elements of Langmuir and Freundlich isotherms which explain equilibrium on homogeneous and heterogeneous surfaces and multilayer adsorption. It possesses three endowments as a_{RP}, K_{RP} and g and is shown by as:

$$q_e = \frac{K_{\text{RP}} C_e}{1 + a_{\text{RP}} C_e^{g}} \tag{16}$$

It is used to show adsorption equilibrium over a wide range of dye concentration molecules. The exponent g lies between 0 and 1. When $\beta = 0$, it becomes Henry's law, and when $\beta = 1$, the Redlich–Peterson equation becomes the Langmuir equation [36].

Sips isotherm was derived for determining the heterogeneous adsorption process and it is a combination of Langmuir and Freundlich isotherms [37]. Nonlinear Sips adsorption isotherm is expressed by the below equation:

$$q_e = \frac{K_S C_e^{\beta}}{1 + a_S C_e^{\beta}} \tag{17}$$

2.6. Adsorption thermodynamic evaluation

Herein, adsorption thermodynamics for MO adsorption onto the commercial anion exchange membrane EPTAC was explored by using the below relationships:

$$\ln K_c = \frac{\Delta S^\circ}{R} - \frac{\Delta H^\circ}{RT} \tag{18}$$

$$K_c = \frac{C_a}{C_e} \tag{19}$$

$$\Delta G^\circ = \Delta H^\circ - T\Delta S^\circ \tag{20}$$

where R, ΔG°, K_c, ΔS° and ΔH° denoted the general gas constant, change in Gibbs free energy (kJ/mol), equilibrium constant, change in entropy (J/mol K) and change in enthalpy (kJ/mol) respectively.

3. Results and discussion

3.1. Effect of operating factors

Fig. 2a depicts the effect of contact time on the percentage removal of MO from wastewater keeping other operating endowments constant. The removal of MO by the commercial anion exchange membrane EPTAC was increased from 26.10% to 98.70% with contact time. Initially, it was fast due to the presence of several empty sites onto the commercial anion exchange membrane EPTAC but it slowed down with the passage of time. It attained saturation in 24 h. It was concluded that equilibrium was obtained within 24 h. Therefore, we employed it for future experiments. Similar results were obtained in our previous work [31]. Keeping the other endowments constant, the influence of membrane dosage onto the percentage removal of MO was revealed and results are given in Fig. 2b. The removal of MO was increased from 48.04% to 98.70% with increasing the membrane dosage because the number of present available active sites onto the commercial anion exchange membrane EPTAC increased. However, further increase in it did not provide any large increase in the removal of MO from aqueous solution. It could be because of the saturation of the commercial anion exchange membrane EPTAC binding sites [31,38]. Fig. 2c represents the influence of the initial concentration of dye solution onto the percentage removal of MO. It was decreased from 83.58% to 16.33% with enhancing initial dye concentration of dye solution. It was associated with a rise in the driving force of concentration gradient to overcome the mass transfer resistance of the dye between the aqueous phases and the solid phases with the increase in the initial concentration [39,40].

Fig. 3a denotes the effect of temperature on the percentage removal of MO from wastewater at room temperature. It was decreased from 98.19% to 78.36% with a rise in temperature from 293 to 323 K. It showed that the removal of MO was an exothermic process. Fig. 3b shows the effect of ionic strength on the percentage removal of MO from wastewater. The removal of MO was declined with enhancing the molarity of NaCl. It was found to be declined from 98.19% to 71.44% with enhancing the molarity of salt NaCl 0.2–1.5 M due to competition between the methyl orange anions and Cl^- for the active sorption sites [41]. Moreover, the mechanism for MO adsorption from wastewater onto anion exchange membrane EPTAC is represented in Fig. 4.

3.2. Adsorption isotherms

Herein, two-parameter isotherms (Langmuir, Freundlich, Temkin and Dubinin–Radushkevich (D–R)) and three-parameter isotherm models (Redlich–Peterson, Hill and Sips) were employed to explain experimental data of MO adsorption onto commercial anion exchange membrane EPTAC from wastewater. Herein, the nonlinear method was endorsed for adsorption isotherm endowment calculation. All the model endowments were studied by

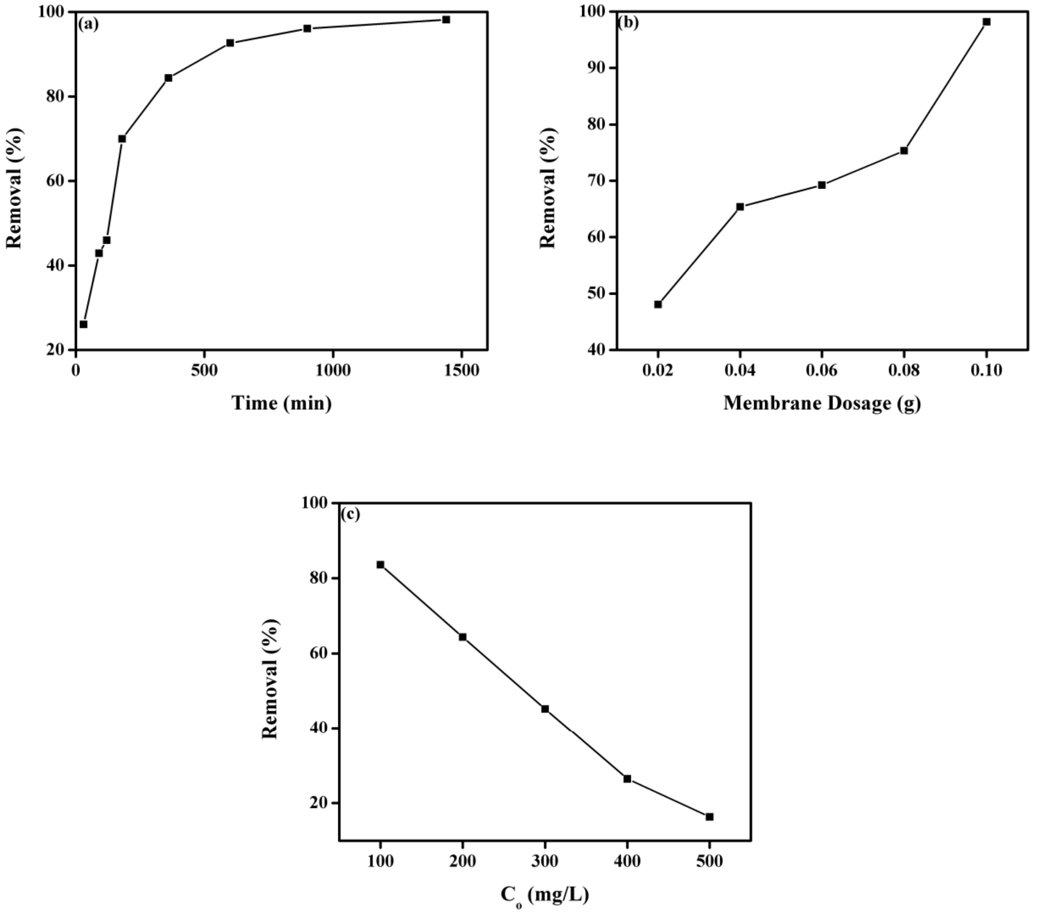

Fig. 2. (a) Effect of contact time, (b) effect of membrane dosage, (c) effect of initial concentration of dye aqueous solution onto adsorptive removal of MO by the commercial anion exchange membranes EPTAC from wastewater.

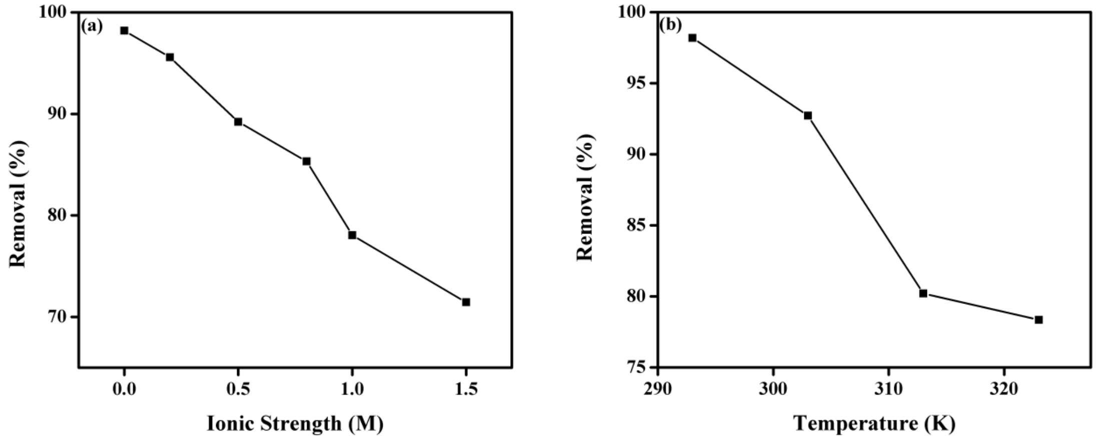

Fig. 3. (a) Effect of ionic strength and (b) temperature on adsorptive removal of MO by the commercial anion exchange membranes EPTAC.

nonlinear regression by using IGOR Pro. Wave Matrices 6.2.1 software [26,42]. The nonlinear chi-square test (χ^2) is a statistical tool needed for the best fit of experimental data and its lower value represents similarities of the experimental data while a large higher denotes variation of experimental data [43].

3.2.1. Two parameters adsorption isotherms

Fig. 5 represents the plot of Langmuir isotherm for adsorption of MO onto the commercial anion exchange membrane EPTAC by nonlinear method and the attained values of Q_m and k_L are given in Table 1. The lower value of the chi-square test (χ^2) (2.76×10^{-8}) represented that adsorption of MO from wastewater onto the commercial anion exchange membrane EPTAC obeyed the Langmuir model. Similarly, the plot of Freundlich isotherm for adsorption of MO onto commercial anion exchange membrane EPTAC by the nonlinear method is denoted in Fig. 5 and the attained values of K_f and n are given in Table 1. The value of the chi-square test (χ^2) is very low (2.22×10^{-9}) exhibited that experimental data for adsorption of MO onto the commercial anion exchange membrane EPTAC obeyed Freundlich isotherm model. The value of Freundlich constant "n" suggested the favourability of the adsorption process whereas K_f is the adsorption capacity of the adsorbent (commercial anion exchange membrane EPTAC). The values of 'n' ranges from 2–10 representing good adsorption, 1–2 moderate adsorption and less than one shows poor adsorption [13]. Fig. 5 depicts the plot of Temkin isotherm for adsorption of MO onto commercial anion exchange membrane EPTAC by nonlinear method and attained values of b_T and a_T are given in Table 1. The lower value of chi-square (7.89×10^{-9}) showed that adsorption of MO onto the commercial anion exchange membrane EPTAC obeyed Temkin isotherm. Moreover, the plot of D–R isotherm for adsorption of MO onto the commercial anion exchange membrane EPTAC by the nonlinear method is shown in Fig. 5. The measured value of mean adsorption energy (E) for adsorption of MO onto the commercial anion exchange membrane EPTAC was 10.55 kJ/mol indicated that adsorption of MO onto the commercial anion exchange membrane EPTAC followed chemical ion-exchange adsorption mechanism. The value of mean adsorption energy (E) in the D–R isotherm can act as a rule to differentiate chemical and physical adsorption [26]. The value of E greater than 8 kJ/mol showed a chemical ion-exchange adsorption process whereas values of E below 8 kJ/mol denoted the physical adsorption process [26].

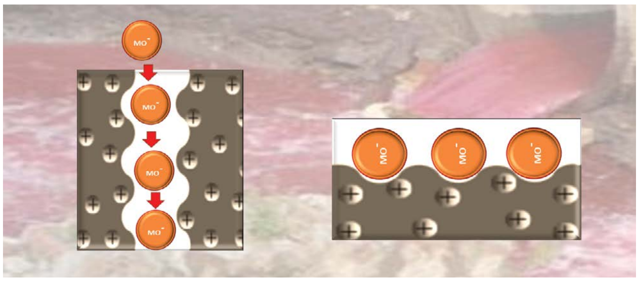

Fig. 4. The proposed mechanism of adsorptive removal of MO by the commercial anion exchange membrane EPTAC from wastewater.

3.2.2. Three parameters adsorption isotherms

Fig. 6 depicts the plot of the Redlich–Peterson model for adsorption MO onto the commercial anion exchange membrane EPTAC from wastewater. It was observed that experimental data followed Redlich–Peterson model with the lower value of χ^2 for adsorption of MO onto the commercial anion exchange membrane EPTAC. The measured endowments of Redlich–Peterson model are given in Table 2. Similarly, the plot of Sips isotherm for adsorption of MO onto the commercial anion exchange membrane EPTAC is indicated in Fig. 6 and the attained value of Sips constants are given in Table 2. The lower value of χ^2 showed that the Sips equation obeyed equilibrium data. Fig. 6 represents the plot of Hill isotherm for adsorption of MO onto the commercial anion exchange membrane

Table 1
Calculated parameters of two parameters isotherm for adsorption of MO onto the commercial anion exchange membranes EPTAC by nonlinear method

Isotherms	Parameters		χ^2
Langmuir isotherm	Q_m	k_L	
	12.44	1.56×10^{-2}	2.76×10^{-8}
Freundlich isotherm	K_f	n	
	4.44×10^{-3}	2.46	2.22×10^{-9}
Temkin isotherm	a_T	b_T	
	6.59×10^{4}	3.63×10^{4}	7.89×10^{-9}
D–R isotherm	Q_m	β	
	2.39×10^{-4}	4.49×10^{-3}	3.42×10^{-9}
	$E = 10.55$ kJ/mol		

Q_m: mg/g; k_L: L/mol; K_f: mol/g; b_T: kJ/mol; a_T: L/mg; β: mol²/J²; C_m: mg/g; E: kJ/mol

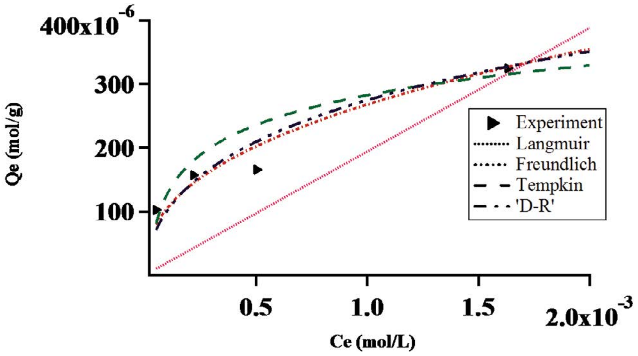

Fig. 5. The plots of two parameters adsorption isotherms for adsorption of MO onto the commercial anion exchange membrane EPTAC by the nonlinear method.

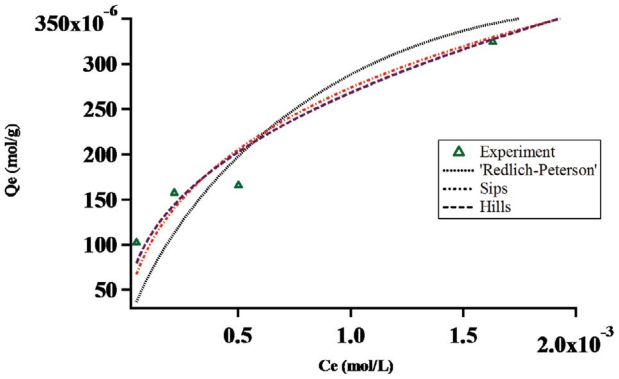

Fig. 6. The plots of three parameters adsorption isotherms for adsorption of MO onto the commercial anion exchange membrane EPTAC by the nonlinear method.

EPTAC and the attained values of its endowments are given in Table 2. The lower value of chi-square indicated that adsorption of MO onto the commercial anion exchange membrane EPTAC can be defined by the Hill model.

3.3. Adsorption kinetics

Fig. 7a denotes the plot of log(q_e – q_t) vs. time for MO adsorption onto the commercial anion exchange membrane EPTAC. The value of k_1 was calculated from the slope of Fig. 7a and given in Table 3. The value of the correlation coefficient (R^2) was 0.994. Further, there was a large difference between experimental adsorption capacity and calculated adsorption capacity, therefore it does not explain the rating process. Moreover, the plot of the pseudo-second-order model for adsorption of MO onto the commercial anion exchange membrane EPTAC is shown in Fig. 7b. The value of adsorption capacity (q_e) can be determined from the slope of Fig. 7b and is given in Table 3. This value was in good agreement with the experimental value (19.63 mg/g). Moreover, the value of the correlation coefficient (R^2) was (R^2 > 0.99) close to unity which showed that experimental data fitted well to the pseudo-second-order model.

Table 2
Determined values of parameters for three parameter isotherms for adsorption of MO onto the commercial anion exchange membranes EPTAC by nonlinear method

Isotherms	Parameters			χ^2
Redlich–Peterson	K_{RP}	a_{RP}	g	
	4.22	–5.17	1.04	8.01 × 10^{-9}
Sips	k_s	β	a_s	
	0.019	0.56	20.45	3.36 × 10^{-9}
Hills	q_h	n_h	k_h	
	1.08	0.41	243.48	2.23 × 10^{-9}

k_s; L/g; a_s: L/g; q_h: mg/g; k_h: (mg)n_h

Fig. 8a indicates the plot Elovich model for adsorption of MO onto the commercial anion exchange membrane EPTAC. The measured values of α and β are given in Table 3. The value of the correlation coefficient (R^2) was 0.872 lower than the pseudo-second-order model. Therefore, it is not convenient to explain the adsorption of MO onto the commercial anion exchange membrane EPTAC. Similarly, the plot of the liquid film diffusion model is shown in Fig. 8b and the calculated value of K_{fd} is given in Table 3. The value of the correlation coefficient (R^2) was lower than the pseudo-second-order model. Hence, it was also not suitable to explain experimental data. The graphical representation of the modified Freundlich model is given in Fig. 8c and the determined values of parameters m and k were are given in Table 3. The value of the

Table 3
Measured values of kinetics parameters for adsorption of MO onto the commercial anion exchange membranes EPTAC

Kinetic models	Parameters		
	$q_{e(exp)}$	19.63	–
Pseudo-first-order model	$q_{e(cal)}$	k_1 × 10^{-3}	R^2
	13.89	1.72	0.994
Pseudo-second-order model	q_e	k_2 × 10^{-4}	R^2
	21.09	4.98	0.995
Elovich model	α	β	R^2
	0.60	0.28	0.872
Liquid film diffusion model	K_{fd} × 10^{-3}	C_{fd}	R^2
	3.97	–0.44	0.940
Modified Freundlich equation	m	k	R^2
	3.09	0.045	0.803
Liquid film diffusion model	k_o	α	R^2
	1.79	0.33	0.805

q_e: mg/g; k_1: (min^{-1}); k_2: g/mg min; α: mg/g min; β: g/mg; K_{fd}: (min^{-1}); k: L/g min; k_o: mL/(g/L)

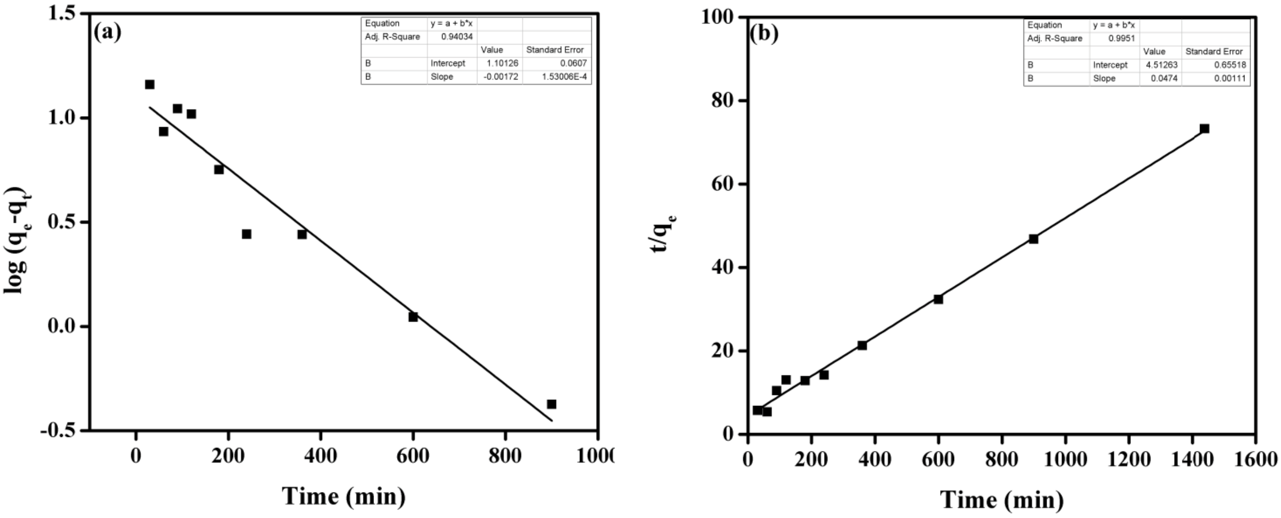

Fig. 7. (a) Pseudo-first-order model and (b) pseudo-second-order kinetics for adsorption of MO onto the commercial anion exchange membrane EPTAC.

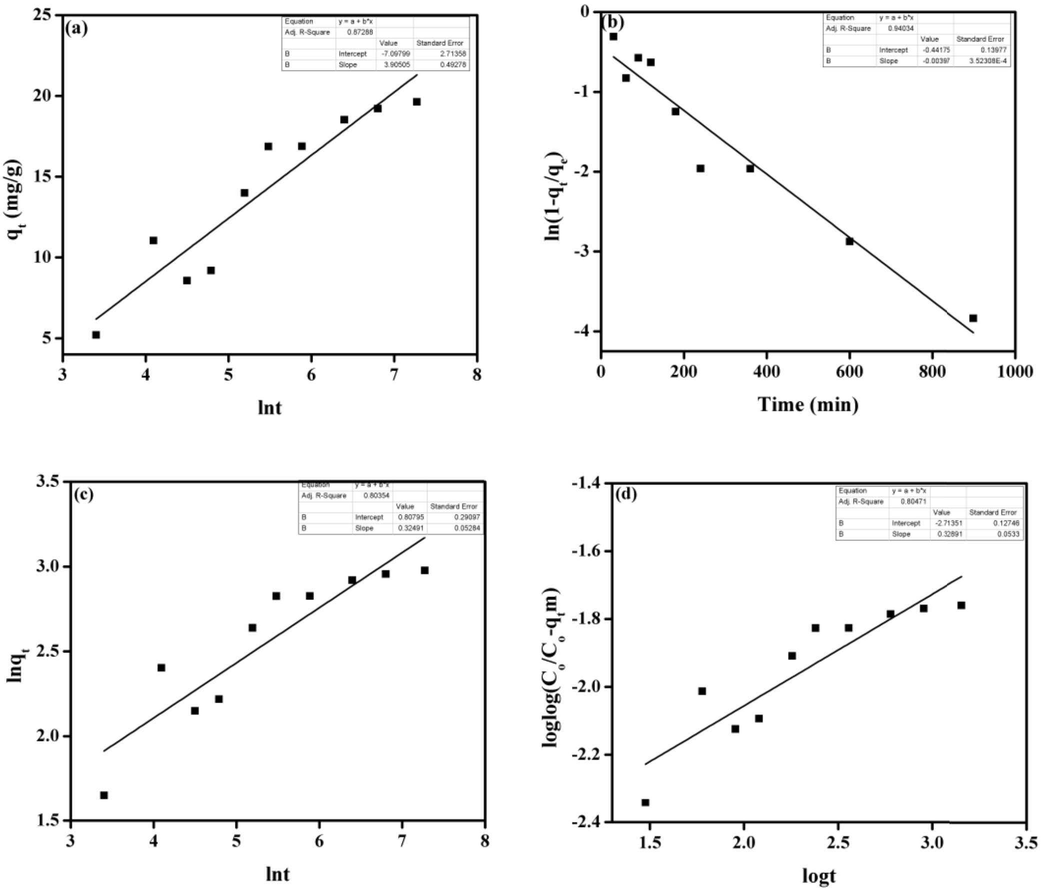

Fig. 8. (a) Elovich model, (b) liquid film diffusion model, (c) modified Freundlich equation, and Bangham equation for adsorption of MO onto the commercial anion exchange membrane EPTAC.

correlation coefficient was 0.803 represented that it is not good to explain the adsorption of MO onto the commercial anion exchange membrane EPTAC. Moreover, the plot of loglog($C_o/C_o - q_t m$) vs. log$t$ for Bangham equation is given in Fig. 8d and the measured values of α and m are given in Table 3. The double logarithmic plot did not give linear curves representing that the diffusion of adsorbate (MO) into pores of the adsorbent (the commercial anion exchange membrane EPTAC) is not the only rate-controlling step [44,45]. It may be that both film and pore diffusion were essential to a different extent for MO adsorption from wastewater onto the commercial anion exchange membrane EPTAC.

3.4. Adsorption thermodynamics

Fig. 9 depicts the plots of lnK_c vs. 1/T for adsorption of MO from wastewater onto the commercial anion exchange membrane EPTAC and the calculated values of thermodynamics factors including change in Gibbs free energy (ΔG°), enthalpy (ΔH°) and entropy (ΔS°) are given in Table 4. The values of Gibbs free energy (ΔG°) was positive at all temperature studied and enhanced from 60.10 to 66.21 kJ/mol with the rise in temperature. It might be because of interaction between adsorbent and adsorbate, with unbalanced competition imputed to the heterogeneity of membrane surface and system got energy from an external source at higher temperatures [28]. The negative value of enthalpy (ΔH° = –68.93 kJ/mol) showed that adsorption of MO onto the commercial anion exchange

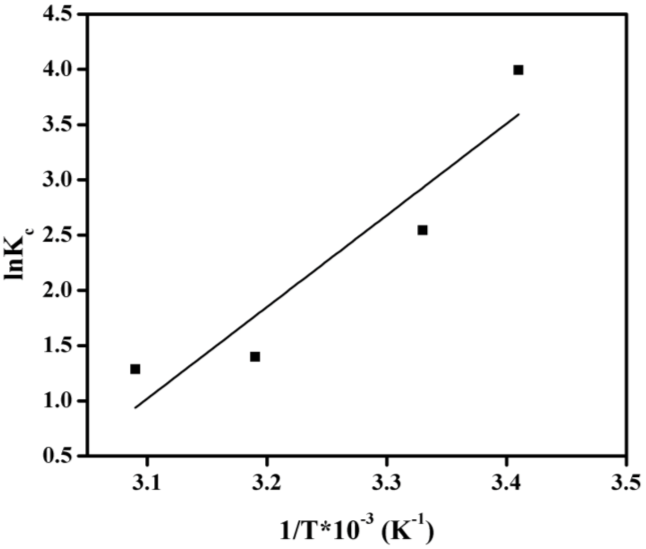

Fig. 9. The plot of 1/T vs. lnK_c for adsorption of MO onto the commercial anion exchange membrane EPTAC.

Table 4
Measured thermodynamic parameters for adsorption of MO onto EPTAC

ΔH° (kJ/mol)	ΔS° (J/mol)	ΔG° (kJ/mol)			
		293 K	303 K	313 K	323 K
–68.93	–205.20	60.10	62.10	64.16	66.21

membrane EPTAC was an exothermic process. Similarly, the negative value of entropy (ΔS° = –205.20 J/mol) showed the decrease in randomness at the adsorbate–adsorbent interface during the adsorption of MO onto the commercial anion exchange membrane EPTAC.

4. Conclusions

In summary, this research showed that the commercial anion exchange membrane EPTAC was useful for the removal of MO from wastewater. The removal of MO was enhanced with contact time and membrane dosage whereas declined with an initial concentration of dye, ionic strength and temperature. Adsorption kinetic study indicated that adsorption of MO onto the commercial anion exchange membrane EPTAC followed pseudo-second-order model because the value of correlation coefficient was close to unity ($R^2 > 0.99$). Adsorption isotherm study showed that experimental data for adsorption of MO on the commercial anion exchange membrane EPTAC obeyed all employed models but best fitted to Freundlich isotherm model. Adsorption thermodynamic study showed that adsorption of MO onto the commercial anion exchange membrane EPTAC was an exothermic process. This research showed that the commercial anion exchange membrane EPTAC could be used as an extraordinary adsorbent for the removal of MO from wastewater at room temperature.

Acknowledgments

The authors are highly thankful to the International Postdoctoral Exchange Fellowship program (Talent-Introduction Program) for financial support.

References

[1] N.M. Mahmoodi, B. Hayati, M. Arami, C. Lan, Adsorption of textile dyes on *Pine Cone* from colored wastewater: kinetic, equilibrium and thermodynamic studies, Desalination, 268 (2011) 117–125.
[2] O. Türgay, G. Ersöz, S. Atalay, J. Forss, U. Welander, The treatment of azo dyes found in textile industry wastewater by anaerobic biological method and chemical oxidation, Sep. Purif. Technol., 79 (2011) 26–33.
[3] I. Gudelj, J. Hrenović, T.L. Dragičević, F. Delaš, V. Šoljan, H. Gudelj, Azo dyes, their environmental effects, and defining a strategy for their biodegradation and detoxification, Arch. Ind. Hyg. Toxicol., 62 (2011) 91–101.
[4] H.Y. He, J.F. Huang, L.Y. Cao, J.P. Wu, Photodegradation of methyl orange aqueous on $MnWO_4$ powder under different light resources and initial pH, Desalination, 252 (2010) 66–70.
[5] G.K. Parshetti, A.A. Telke, D.C. Kalyani, S.P. Govindwar, Decolorization and detoxification of sulfonated azo dye methyl orange by Kocuria rosea MTCC 1532, J. Hazard. Mater., 176 (2010) 503–509.
[6] L. Gomathi Devi, K. Mohan Reddy, Enhanced photocatalytic activity of silver metallized TiO_2 particles in the degradation of an azo dye methyl orange: characterization and activity at different pH values, Appl. Surf. Sci., 256 (2010) 3116–3121.
[7] M.-Y. Teng, S.-H. Lin, Removal of methyl orange dye from water onto raw and acidactivated montmorillonite in fixed beds, Desalination, 201 (2006) 71–81.
[8] J.B. Weber, C.T. Miller, Organic chemical movement over and through soil, React. Mov. Org. Chem. Soils, 22 (1989) 305–334.
[9] M. Doğan, M.H. Karaoğlu, M. Alkan, Adsorption kinetics of maxilon yellow 4GL and maxilon red GRL dyes on kaolinite, J. Hazard. Mater., 165 (2009) 1142–1151.
[10] M. Hamdi Karaoğlu, M. Doğan, M. Alkan, Removal of cationic dyes by kaolinite, Microporous Mesoporous Mater., 122 (2009) 20–27.
[11] P. Girods, A. Dufour, V. Fierro, Y. Rogaume, C. Rogaume, A. Zoulalian, A. Celzard, Activated carbons prepared from wood particleboard wastes: characterisation and phenol adsorption capacities, J. Hazard. Mater., 166 (2009) 491–501.
[12] S. Zafar, M.I. Khan, M. Khraisheh, S. Shahida,T. Javed, M.L. Mirza, N. Khalid, Use of rice husk as an efective sorbent for the removal of cerium ions from aqueous solution: kinetic, equilibrium and thermodynamic studies, Desal. Water Treat., 150 (2019) 124–135.
[13] S. Zafar, M.I. Khan, M. Khraisheh, M.H. Lashari, S. Shahida, M.F. Azhar, P. Prapamonthon, M.L. Mirza, N. Khalid, Kinetic, equilibrium and thermodynamic studies for adsorption of nickel ions onto husk of *Oryza sativa*, Desal. Water Treat., 167 (2019) 277–290.
[14] S. Zafar, M.I. Khan, M. Khraisheh, S. Shahida, N. Khalid, M.L. Mirza,, Effective removal of lanthanum ions from aqueous solution using rice husk: impact of experimental variables, Desal. Water Treat., 132 (2018) 263–273.
[15] M.I. Khan, S. Zafar, M.A. Khan, F. Mumtaz, P. Prapamonthon, A.R. Buzdar, Bougainvillea glabra leaves for adsorption of congo red from wastewater, Fresenius Environ. Bull., 27 (2018) 1456–1465.
[16] M.I. Khan, S. Zafar, M.F. Azhar, A.R. Buzdar, W. Hassan, A. Aziz, M. Khraisheh, Leaves powder of syzgium cumini as an adsorbent for removal of congo red dye from aqueous solution, Fresenius Environ. Bull., 27 (2018) 3342–3350.
[17] M.I. Khan, S. Zafar, A.R. Buzdar, M.F. Azhar, W. Hassan, A. Aziz, Use of citrus sinensis leaves as a bioadsorbent for removal of congo red dye from aqueous solution, Fresenius Environ. Bull., 27 (2018) 4679–4688.
[18] M.I. Khan, S. Zafar, H.B. Ahmad, M. Hussain, Z. Shafiq, Use of morus albal leaves as bioadsorbent for the removal of congo red dye, Fresenius Environ. Bull., 24 (2015) 2251–2258.
[19] B.H. Hameed, I.A.W. Tan, A.L. Ahmad, Adsorption isotherm, kinetic modeling and mechanism of 2,4,6-trichlorophenol on coconut husk-based activated carbon, Chem. Eng. J., 144 (2008) 235–244.
[20] R. Jain, M. Shrivastava, Adsorptive studies of hazardous dye Tropaeoline 000 from an aqueous phase on to coconut-husk, J. Hazard. Mater., 158 (2008) 549–556.
[21] M.M. Nassar, K.T. Awida, E.E. Ebrahiem, Y.H. Magdy, M.H. Mehaedi, Fixed-bed adsorption for the removal of iron and manganese onto palm fruit bunch and maize cob, Adsorpt. Sci. Technol., 21 (2003) 161–175.
[22] C. Namasivayam, S. Sumithra, Adsorptive removal of phenols by Fe(III)/Cr(III) hydroxide, an industrial solid waste, Clean Technol. Environ. Policy, 9 (2007) 215–223.
[23] C.-H. Liu, J.-S. Wu, H.-C. Chiu, S.-Y. Suen, K.H. Chu, Removal of anionic reactive dyes from water using anion exchange membranes as adsorbers, Water Res., 41 (2007) 1491–1500.
[24] S. Zafar, M.I. Khan, H. Rehman, J. Fernandez-Garcia, S. Shahida, P. Prapamonthon, M. Khraisheh, A. Rehman, H.B. Ahmad, M.L. Mirza, N. Khalid, M.H. Lashari, Kinetic, equilibrium, and thermodynamic studies for adsorptive removal of cobalt ions by rice husk from aqueous solution, Desal. Water Treat., 204 (2020) 285–296.
[25] S. Zafar, M.I. Khan, M.H. Lashari, M. Khraisheh, F. Almomani, M.L. Mirza, N. Khalid, Removal of copper ions from aqueous

solution using NaOH-treated rice husk, Emergent Mater., 3 (2020) 857–870.

[26] M.I. Khan, M.H. Lashari, M. Khraisheh, S. Shahida, S. Zafar, P. Prapamonthon, A. ur Rehman, S. Anjum, N. Akhtar, F. Hanif, Adsorption kinetic, equilibrium and thermodynamic studies of Eosin-B onto anion exchange membrane, Desal. Water Treat., 155 (2019) 84–93.

[27] M.I. Khan, S. Zafar, M.A. Khan, A.R. Buzdar, P. Prapamonthon, Adsorption kinetic, equilibrium and thermodynamic study for the removal of congo red from aqueous solution, Desal. Water Treat., 98 (2017) 294–305.

[28] M.A. Khan, M.I. Khan, S. Zafar, Removal of different anionic dyes from aqueous solution by anion exchange membrane, Membr. Water Treat., 8 (2017) 259–277.

[29] M.I. Khan, M.A. Khan, S. Zafar, M.N. Ashiq, M. Athar, A.M. Qureshi, M. Arshad, Kinetic, equilibrium and thermodynamic studies for the adsorption of methyl orange using new anion exchange membrane (BII), Desal. Water Treat., 58 (2017) 285–297.

[30] M.I. Khan, J. Su, L. Guo, Development of triethanolamine functionalized-anion exchange membrane for adsorptive removal of methyl orange from aqueous solution, Desal. Water Treat., 209 (2021) 342–352.

[31] M.I. Khan, A. Shanableh, J. Fernandez, M.H. Lashari, S. Shahida, S. Manzoor, S. Zafar, A. ur Rehman, N. Elboughdiri, Synthesis of DMEA-grafted anion exchange membrane for adsorptive discharge of methyl orange from wastewaters, Membranes, 11 (2021) 166, doi: 10.3390/membranes11030166.

[32] M.I. Khan, L. Wu, A.N. Mondal, Z. Yao, L. Ge, T. Xu, Adsorption of methyl orange from aqueous solution on anion exchange membranes: adsorption kinetics and equilibrium, Membr. Water Treat., 7 (2016) 23–38.

[33] M.I. Khan, T.M. Ansari, S. Zafar, A.R. Buzdar, M.A. Khan, F. Mumtaz, Prasert Prapamonthon, Mehwish Akhtar, Acid green-25 removal from wastewater by anion exchange membrane: adsorption kinetic and thermodynamic studies, Membr. Water Treat., 9 (2018) 79–85.

[34] M.I. Khan, S. Akhtar, S. Zafar, A. Shaheen, M.A. Khan, R. Luque, A. Rehman, Removal of congo red from aqueous solution by anion exchange membrane (EBTAC): adsorption kinetics and themodynamics, Materials, 8 (2015) 4147–4161.

[35] S. Chen, Q. Yue, B. Gao, Q. Li, X. Xu, Removal of Cr(VI) from aqueous solution using modified corn stalks: characteristic, equilibrium, kinetic and thermodynamic study, Chem. Eng. J., 168 (2011) 909–917.

[36] M. Brdar, M. Šćiban, A. Takači, T. Došenović, Comparison of two and three parameters adsorption isotherm for Cr(VI) onto Kraft lignin, Chem. Eng. J., 183 (2012) 108–111.

[37] R. Sips, Combined form of Langmuir and Freundlich equations, J. Phys. Chem., 16 (1948) 490–495.

[38] S. Mohan, R. Gandhimathi, Removal of heavy metal ions from municipal solid waste leachate using coal fly ash as an adsorbent, J. Hazard. Mater., 169 (2009) 351–359.

[39] L. Ai, H. Huang, Z. Chen, X. Wei, J. Jiang, Activated carbon/$CoFe_2O_4$ composites: facile synthesis, magnetic performance and their potential application for the removal of malachite green from water, Chem. Eng. J., 156 (2010) 243–249.

[40] L. Ai, J. Jiang, Fast removal of organic dyes from aqueous solutions by AC/ferrospinel composite, Desalination, 262 (2010) 134–140.

[41] R. Gong, Y. Ding, M. Li, C. Yang, H. Liu, Y. Sun, Utilization of powdered peanut hull as biosorbent for removal of anionic dyes from aqueous solution, Dyes Pigm., 64 (2005) 187–192.

[42] S. Zafar, N. Khalid, M. Daud, M.L. Mirza, Kinetic studies of the adsorption of thorium ions onto rice husk from aqueous media: linear and nonlinear approach, The Nucleus, 52 (2015) 14–19.

[43] M.C. Ncibi, Applicability of some statistical tools to predict optimum adsorption isotherm after linear and non-linear regression analysis, J. Hazard. Mater., 153 (2008) 207–212.

[44] E. Tütem, R. Apak, Ç.F. Ünal, Adsorptive removal of chlorophenols from water by bituminous shale, Water Res., 32 (1998) 2315–2324.

[45] I.D. Mall, V.C. Srivastava, N.K. Agarwal, I.M. Mishra, Adsorptive removal of malachite green dye from aqueous solution by bagasse fly ash and activated carbon-kinetic study and equilibrium isotherm analyses, Colloids Surf., A, 264 (2005) 17–28.